Electronic Supplementary Material (ESI) for Green Chemistry.
This journal is © The Royal Society of Chemistry 2018

- Supporting information -

Supported Gold- and Silver-based Catalysts for the Selective Aerobic Oxidation of 5-(Hydroxymethyl)furfural to 2,5-Furandicarboxylic acid and 5-Hyroxymethyl-2-furancarboxylic acid

O. R. Schade, [†,‡] K. F. Kalz, [†,‡] D. Neukum, [‡] W. Kleist, [§] and J.-D. Grunwaldt [†,‡ *]

[†] *Institute for Chemical Technology and Polymer Chemistry, Karlsruhe Institute of Technology (KIT), 76131 Karlsruhe, Germany*

[‡] *Institute of Catalysis Research and Technology, Karlsruhe Institute of Technology (KIT), 76344 Eggenstein-Leopoldshafen, Germany*

[§] *Industrial Chemistry – Nanostructured Catalyst Materials, Ruhr-University Bochum, 44801 Bochum, Germany*

Table of contents

* Corresponding author: grunwaldt@kit.edu

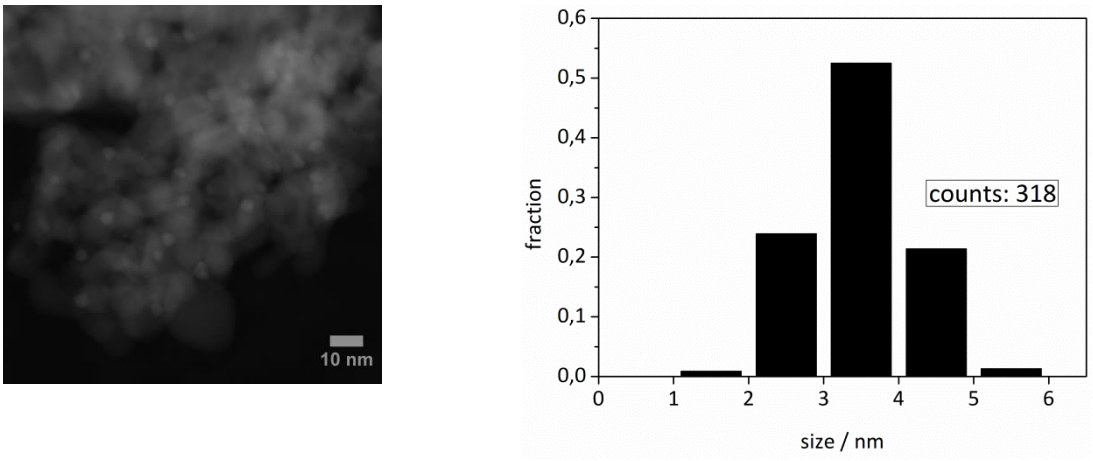

Figure S 1: TEM image and particle size distribution of the Au/ZrO_2_dp catalyst.

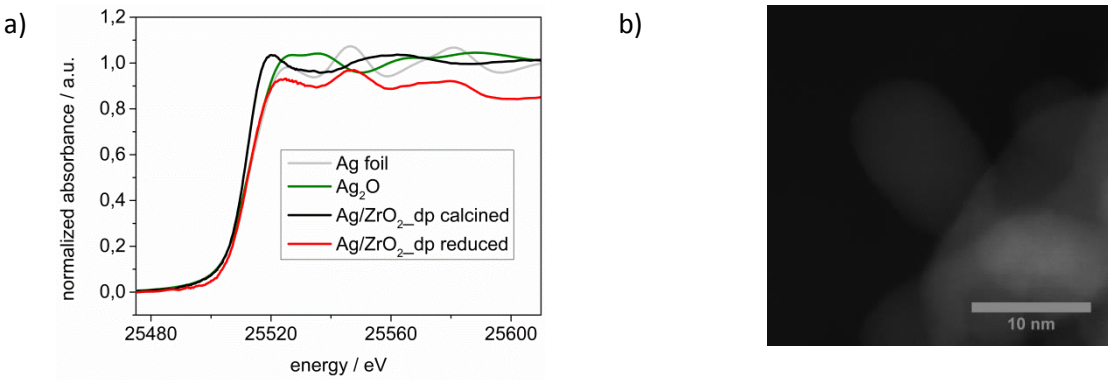

Figure S 2: Characterization of the Ag/ZrO_2_dp catalyst via a) XAS at the Ag-K edge and b) HRTEM of the reduced catalyst.

Since no distinct silver particles were visible in TEM images of the Ag/ZrO_2_dp catalyst, this catalyst was characterized using further methods. Figure S2a shows the X-ray absorption near edge spectra of the calcined and the reduced catalyst together with representative reference compounds. X-ray absorption spectra were measured at the CAT-ACT beamline at KIT synchrotron in Karlsruhe, Germany (2.5 GeV ring, 100-150 mA) using a double crystal monochromator with a pair of Si(311) crystals. Higher harmonics were rejected by a pair of Rh coated Si mirrors and ionization chambers were used to determine X-ray intensities of the incoming beam, behind the sample and behind the silver reference foil. For this purpose, the undiluted catalyst was pressed as a pellet and absorption was measured in transmission mode at the Ag-K edge and a beam size of 1 mm in height and width. Metallic silver foil (Ag K-edge at 25514 eV) was used for energy calibration and the data were normalized. From the XANES region it can be seen that silver was in an oxidized state after calcination and in metallic state after reduction. Since TEM was measured on the reduced catalyst, the reason for no visible particles in TEM might therefore be attributed to the low metal loading and the low contrast between silver and the support material. Therefore, the catalyst was further characterized using HRTEM (Figure S2b) which revealed the presence of some elliptical particles with a size of about 5 nm.

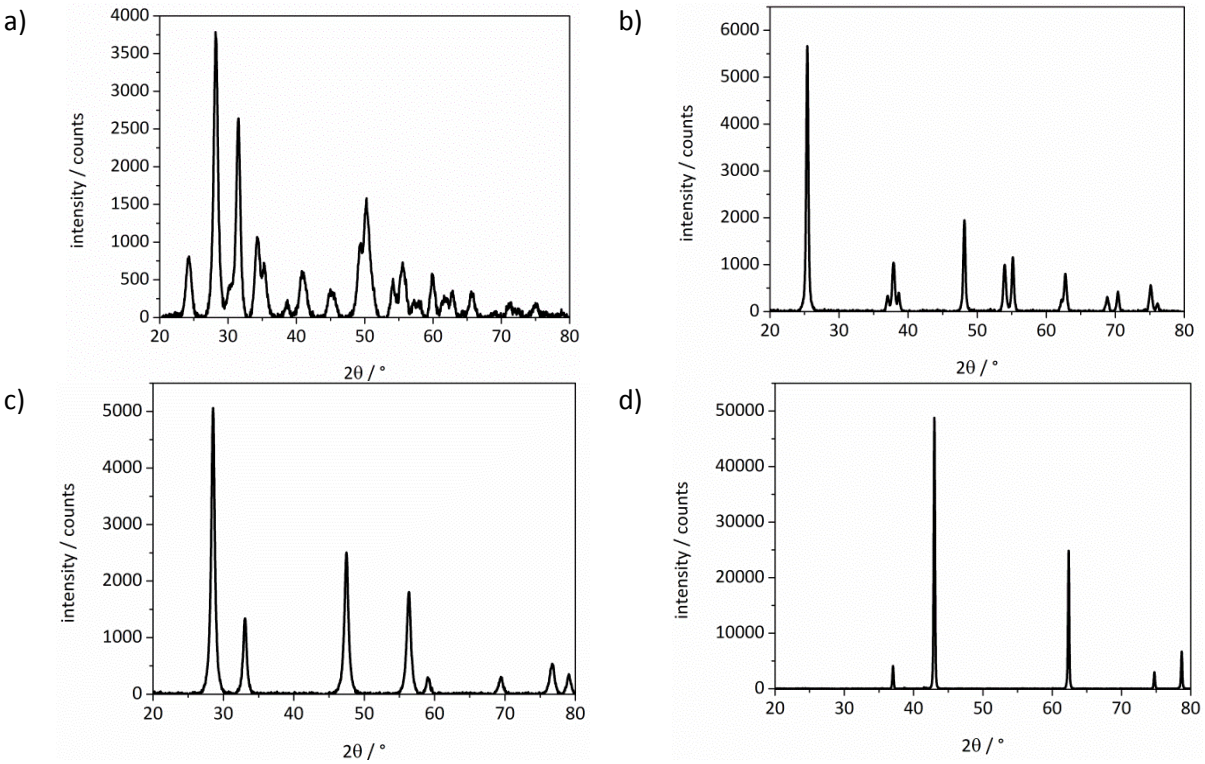

Figure S 3: XRD patterns of the a) ZrO_2, b) TiO_2, c) CeO_2 and d) MgO support materials.

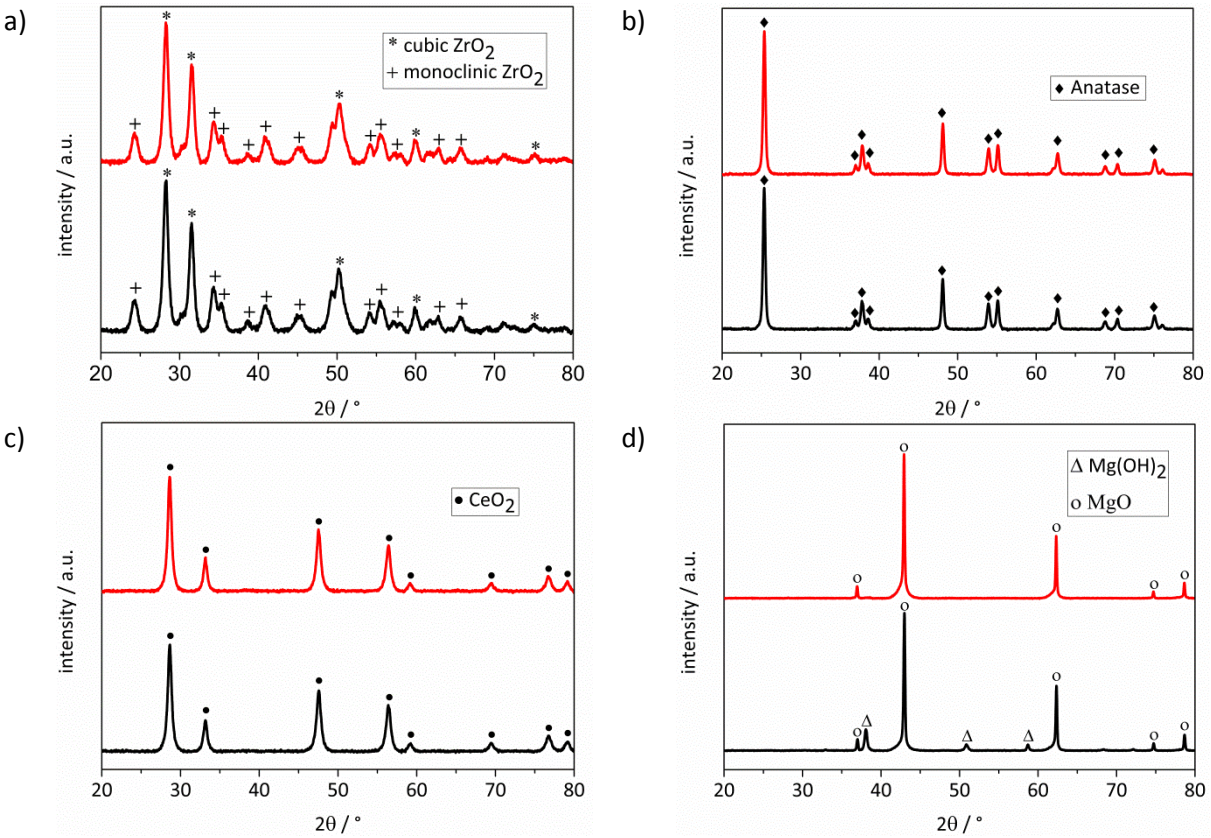

Figure S 4: XRD patterns of a) Au/ZrO_2_dp, b) Au/TiO_2_dp, c) Au/CeO_2_dp and d) Au/MgO_dp catalysts. Black lines correspond to calcined catalysts, red lines represent reduced catalysts.

No changes were observed in the XRD patterns of the Au catalysts on different support materials. However, for the Au catalyst supported on MgO, reflections of $Mg(OH)_2$ emerged after calcination which disappeared upon reduction.

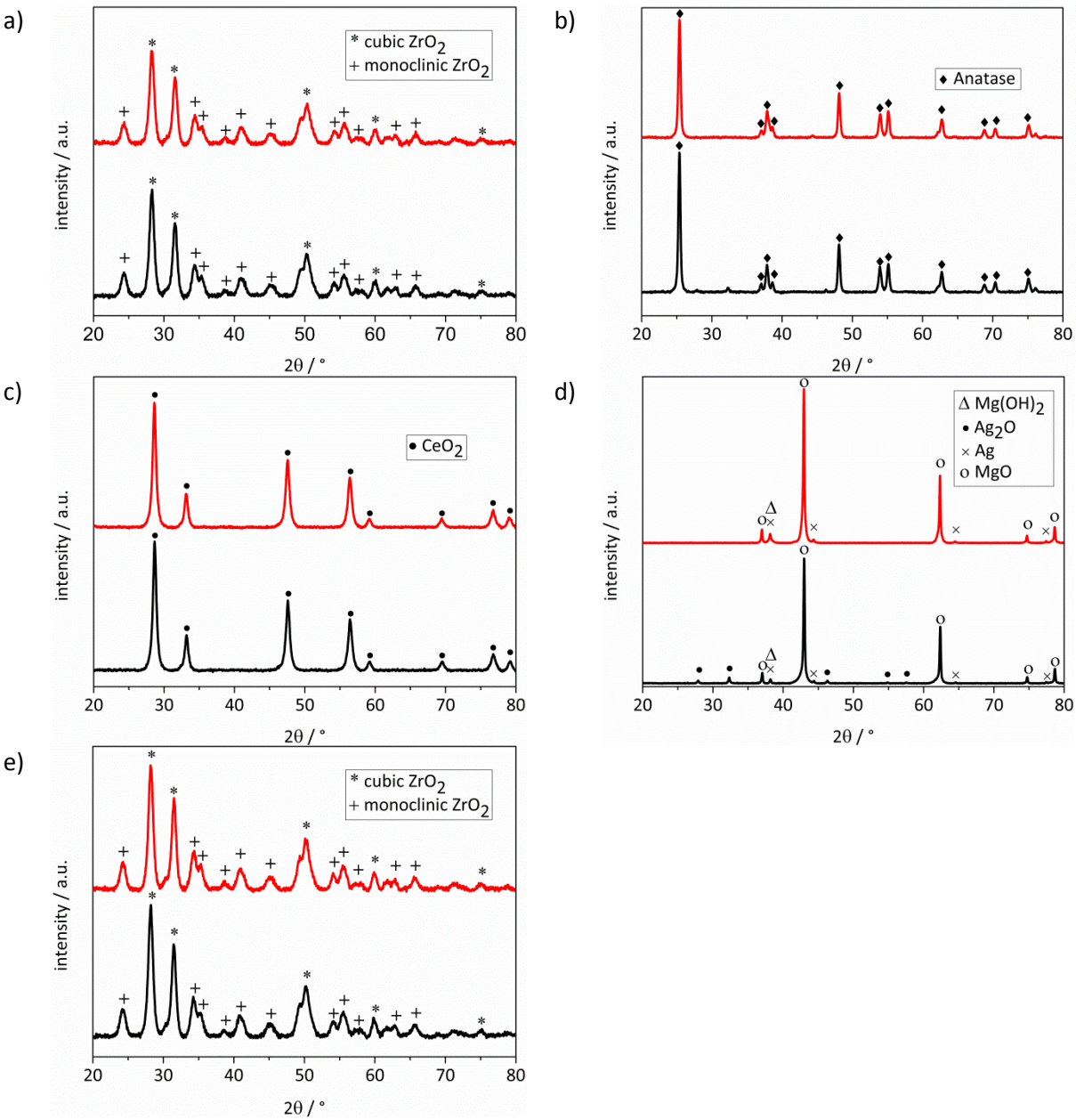

Figure S 5: XRD patterns of a) Ag/ZrO_2_dp, b) Ag/TiO_2_dp, c) Ag/CeO_2_dp, d) Ag/MgO_dp and e) Ag/ZrO_2_imp catalysts. Black lines correspond to calcined catalysts, red lines represent reduced catalysts.

As in the case of Au catalysts, no reflections of noble metals were observed for the Ag catalysts on different support materials except for the catalyst supported on MgO. Reflections from both Ag_2O and Ag were found for the calcined catalyst, which disappeared upon reduction in the case of Ag_2O.

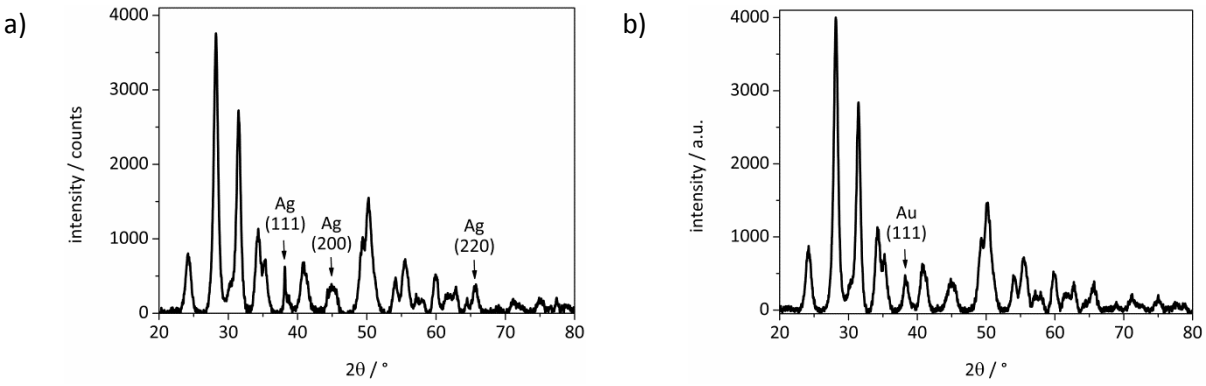

Figure S 6: XRD patterns of spent a) Ag/ZrO_2_dp and b) Au/ZrO_2_dp catalysts.

For both catalysts, reflections of noble metals were found in the XRD patterns of spent catalysts. This indicates a growth in particle size which might be a reason for a decreasing activity in the recycling experiments with both catalysts.

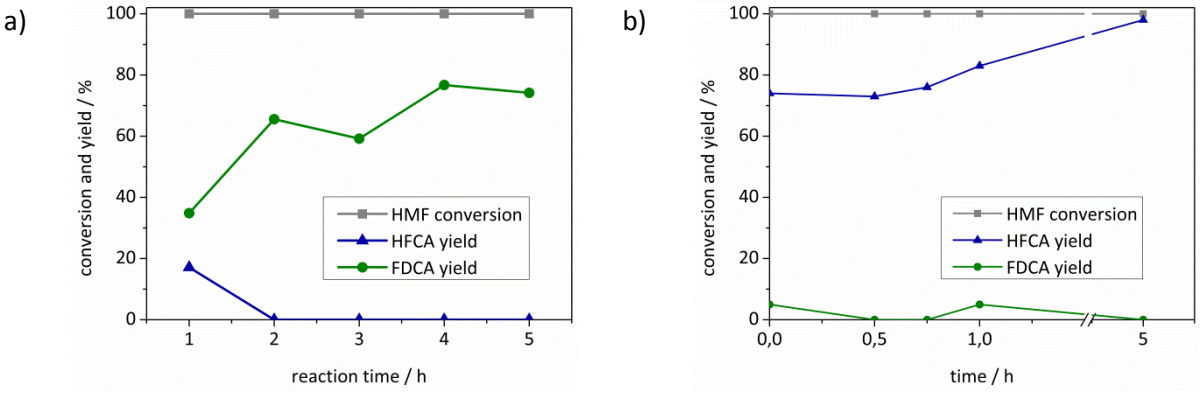

Figure S 7: Time dependent conversion and product distributions using a) Au/ZrO_2_dp and b) Ag/ZrO_2_dp. Reaction conditions: a) 125 °C, 10 bar air pressure, 4 equivalents NaOH, 1 mmol HMF in 10 mL H_2O, 98 mg Au/ZrO_2_dp catalyst. b) 50 °C, 4 equivalents NaOH, 1 mmol HMF in 10 mL H_2O, 54 mg Ag/ZrO_2_dp catalyst.

For both catalysts increasing product yields were observed with longer reaction times. Note that, as stated in the experimental section of the main publication, the starting point of reactions was set after the desired reaction temperature was reached for the first time. Therefore, HMF was already converted at the starting point of the reactions. For the Au/ZrO_2_dp catalyst (Figure S 7a), low yields of oxidation products were obtained after one hour of reaction time at full HMF conversion. While no HFCA was present in the reaction solution after two hours reaction time, the FDCA yield was still increasing. This has also been observed in other studies[1] and might be attributed to product molecules still being adsorbed on the solid catalysts. Also the HFCA yield increased with longer reaction time using Ag/ZrO_2_dp (Figure S 6b), however, the HFCA yield was already above 70 % at the starting point of the reaction showing a very rapid oxidation of the aldehyde moiety.

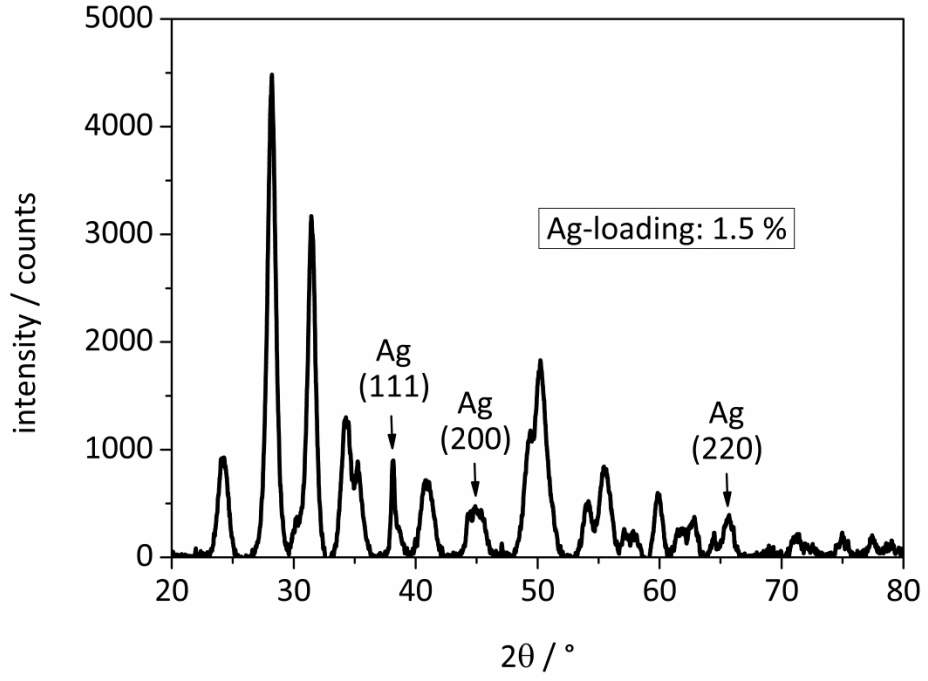

Figure S 8: XRD pattern of the resulting solid after the test reaction using $AgNO_3$ and pure ZrO_2 support.

In the model experiment, pure ZrO_2 support and $AgNO_3$ were used for the oxidation of HMF. The resulting solid was characterized via XRF and XRD after the reaction. XRF confirmed the presence of silver (1.5 wt%) on the ZrO_2 support. In addition, sharp reflections of silver were found in the XRD pattern indicating the presence of large silver particles.

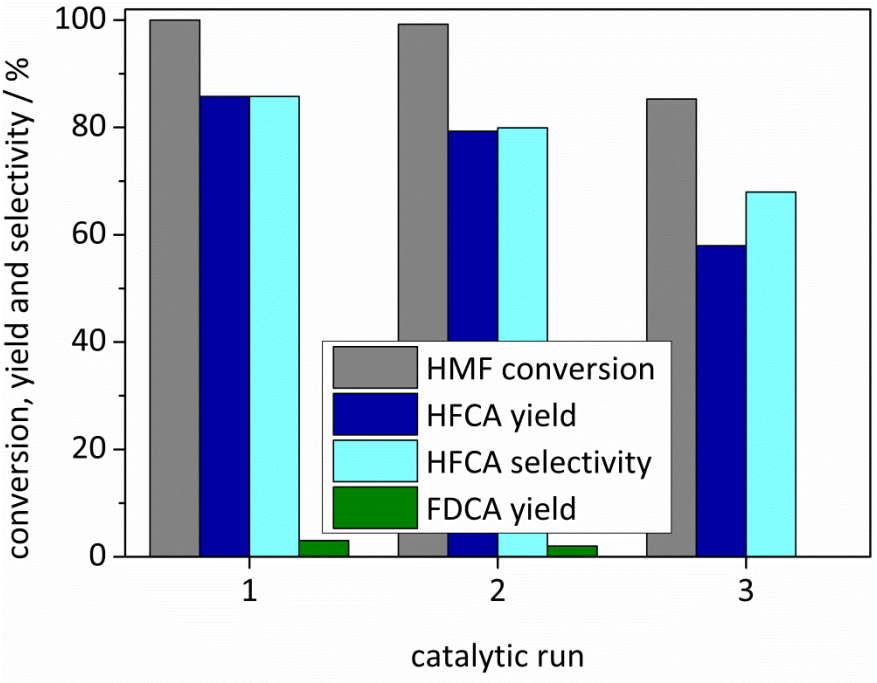

Figure S 9: Stability tests of the Ag/ZrO_2_cp_500 catalyst. Reaction conditions: 50 °C, 10 bar air pressure, 4 equivalents NaOH, 1 h reaction time, HMF and H_2O adjusted to recovered catalyst.

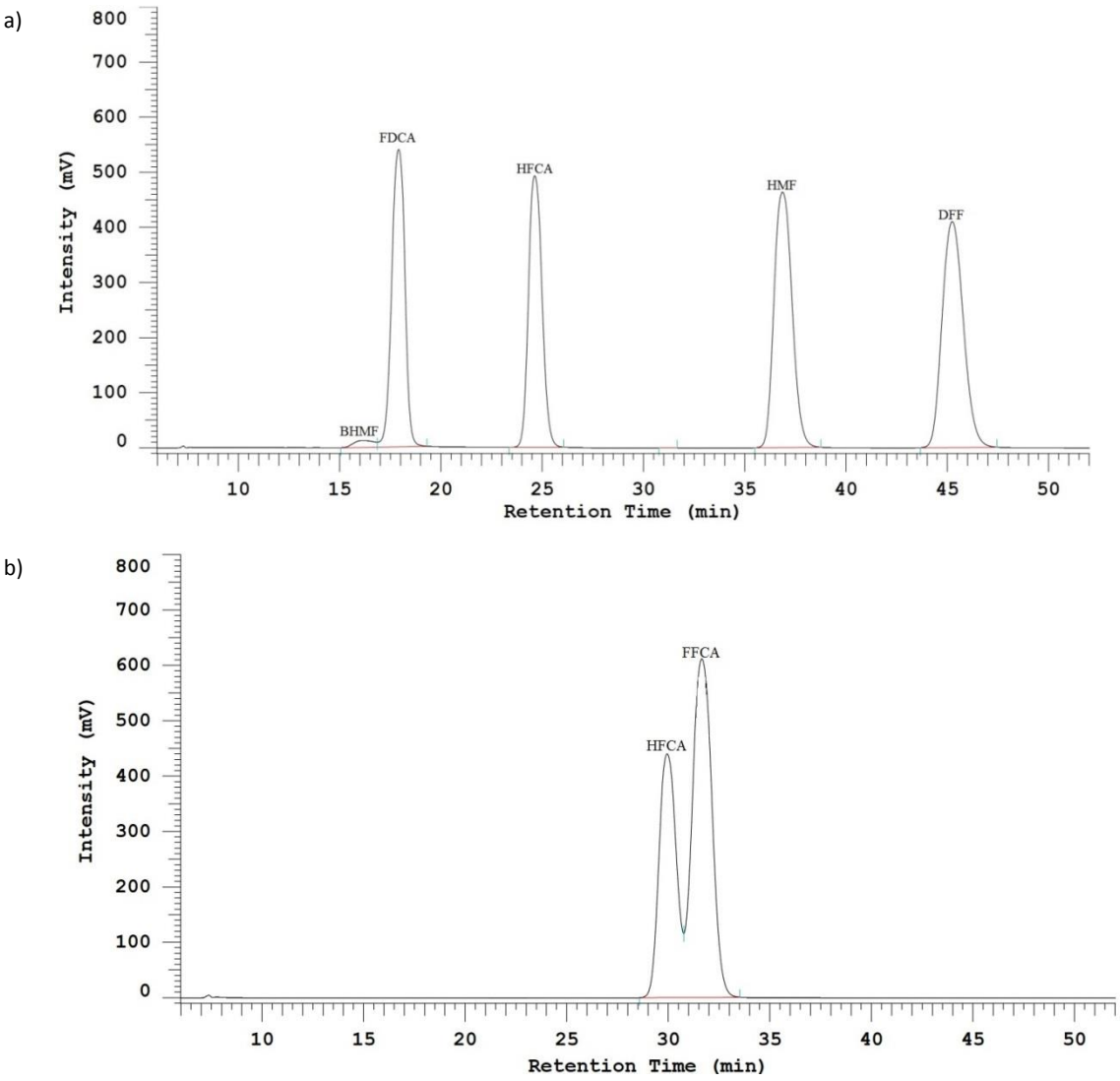

Figure S 10: HPLC chromatograms of reference compounds representing possible HMF oxidation products.

Two settings were used for the characterization of product solutions where all possible oxidation products of HMF were calibrated. Basic HPLC measurements were performed as described in the original publication. However, the peaks of HFCA and another possible oxidation product, FFCA, slightly overlapped with this method. Therefore, reaction solutions where HFCA was present were also measured at a lower temperature of 25 °C, where those products could be measured. However, in none of the experiments performed in this study, FFCA was detected indicating a rapid conversion of aldehydes over catalysts active in FDCA synthesis.

Table S 1: Blank experiments of HMF degradation in basic aqueous solution. Reaction conditions: 10 bar air pressure, 4 equivalents NaOH, 5 h reaction time, 1 mmol HMF in 10 mL H_2O.

Temperature	HMF conversion	HFCA yield	HFCA selectivity	FDCA yield	FDCA selectivity
50 °C	96 %	30 %	32 %	4 %	4 %
100 °C	100 %	5 %	5 %	2 %	2 %

Table S 2: Catalytic tests using leaching solutions of the Ag/ZrO_2_dp catalyst. Reaction conditions: 50 °C, 10 bar air pressure, 1 h reaction time, 1 mmol HMF in 10 mL of the corresponding leaching solution.

pH	HMF conversion	HFCA yield	HFCA selectivity	FDCA yield	FDCA selectivity
8	0 %	-	-	-	-
12	0 %	-	-	-	-
14	62 %	15 %	24 %	1 %	2 %

To investigate the leaching of silver and a possible contribution of homogeneous catalysis, model experiments were performed. The catalysts were treated under reaction conditions at different pH values, but in the absence of HMF as a reducing agent, to gain insight into the leaching behavior of Ag/ZrO_2_dp. After reaction, the catalyst was filtered off and HMF was added to the solution. HMF was not converted using the solutions with an initial pH of 8 and 10, respectively. However, HMF was converted using the solution with an initial pH = 14, but HFCA was produced with a low selectivity. Those results show that leached silver was active to some extent at high pH but the low selectivity and further tests (cf. original publication) indicated a predominantly heterogeneous mechanism.

Table S 3: FDCA productivity calculated for different monometallic gold-based catalysts described in literature.

Reference	Catalyst	FDCA yield	Moles of Au	Reaction time	Productivity / $mol_{FDCA} \cdot mol_{Au}^{-1} \cdot h^{-1}$
[2]	Au/CeO_2	96 %	$4.7 \cdot 10^{-7}$ mol	5 h	123
[3]	Au/TiO_2	71 %	$1.0 \cdot 10^{-5}$ mol	18 h	4
[4]	Au/HT	99 %	$2.5 \cdot 10^{-5}$ mol	7 h	6
[5]	Au/HY	98 %	$2.3 \cdot 10^{-5}$ mol	6 h	18
[6]	$Au/Ce_{0.9}Bi_{0.1}O_{2-\delta}$	99 %	$6.0 \cdot 10^{-6}$ mol	2 h	74
[7]	Au/HT-AC	99 %	$5.0 \cdot 10^{-6}$ mol	12 h	8

FDCA productivity was calculated for some publications where monometallic Au catalysts have been used for the oxidation of HMF. However, comparability is limited due to the different reaction conditions applied in those studies (e.g. temperature or presence of base).

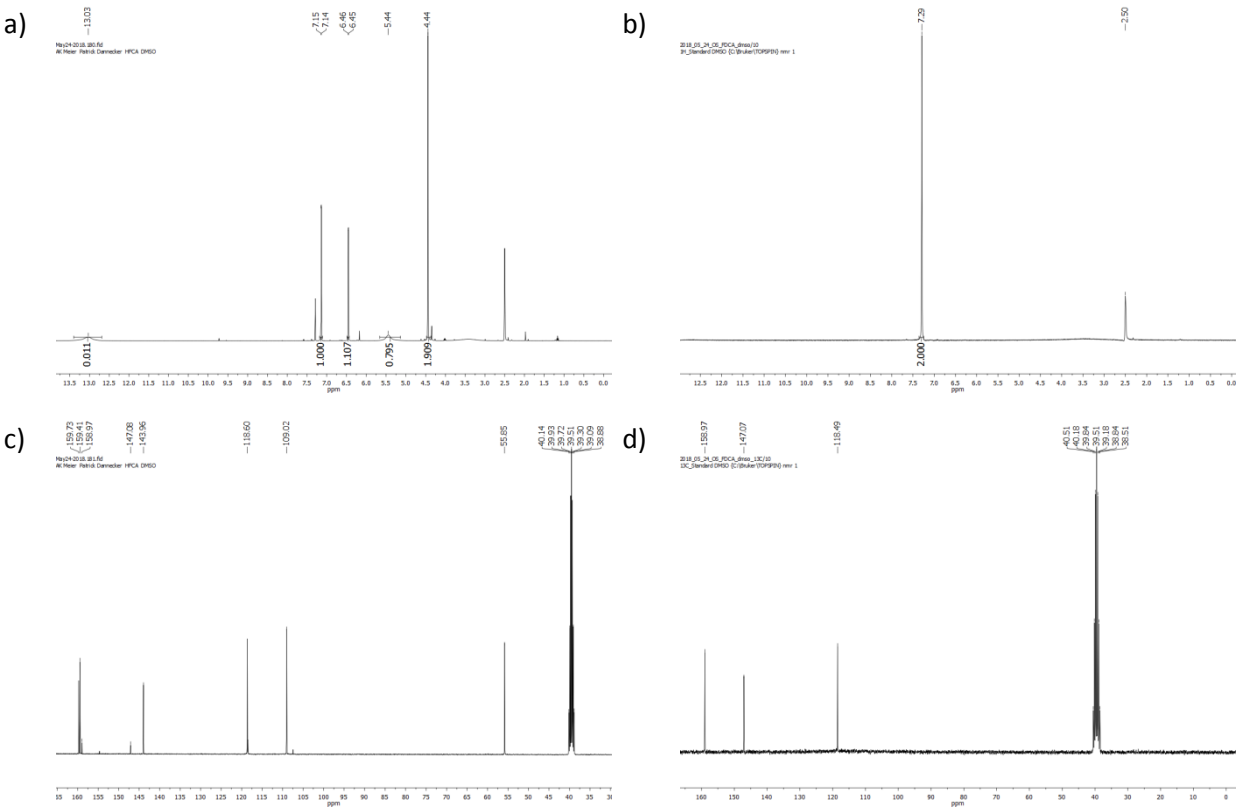

Figure S 11: ^{1}H NMR spectra of a) HFCA and b) FDCA and ^{13}C NMR spectra of c) HFCA and d) FDCA separated from the reaction solutions.

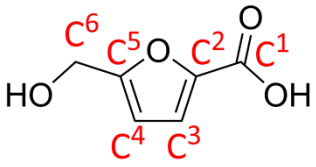

HFCA

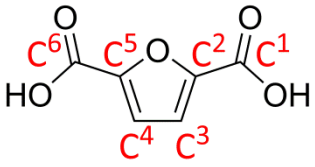

FDCA

<u>HFCA</u>

^{1}H NMR (400 MHz, DMSO-d_6, 300 K): 13.03 (sbr, 1 H, COOH), 7.15 (d, J=7.14 Hz, 1 H, C^3-H), 6.45 (d, J=6.45 Hz, 1 H, C^4-H), 5.44 (sbr, 1 H, OH), 4.44 (s, 2 H, C^6-H_2); ^{13}C NMR (100 MHz, DMSO-d_6, 300 K): 159.73 (C^1), 159.41 (C^5), 143.96 (C^2), 118.60 (C^3), 109.02 (C^4), 55.85 (C^6).

<u>FDCA</u>

^{1}H NMR (250 MHz, DMSO-d_6, 298 K): 7.29 (s, 2 H, C^3/C^4-H); ^{13}C NMR (63 MHz, DMSO-*d6*, 298 K): 158.97 (C^1, C^6), 147.07 (C^2, C^5), 118.49 (C^3, C^4).

Figure S11 shows representative ^{1}H and ^{13}C NMR spectra of HFCA and FDCA which were separated from reaction solutions with a product yield of 80 % or higher. For details on product separation see main publication.

References

1. J. Shen, H. Chen, K. Chen, Y. Qin, X. Lu, P. Ouyang and J. Fu, *Ind. Eng. Chem. Res.*, 2018.
2. O. Casanova, S. Iborra and A. Corma, *ChemSusChem*, 2009, **2**, 1138-1144.
3. Y. Y. Gorbanev, S. K. Klitgaard, J. M. Woodley, C. H. Christensen and A. Riisager, *ChemSusChem*, 2009, **2**, 672-675.

4. N. K. Gupta, S. Nishimura, A. Takagaki and K. Ebitani, *Green Chem.*, 2011, **13**, 824-827.
5. J. Cai, H. Ma, J. Zhang, Q. Song, Z. Du, Y. Huang and J. Xu, *Chem. Eur. J.*, 2013, **19**, 14215-14223.
6. Z. Miao, Y. Zhang, X. Pan, T. Wu, B. Zhang, J. Li, T. Yi, Z. Zhang and X. Yang, *Catal. Sci. Technol.*, 2015, **5**, 1314-1322.
7. T. Gao, T. Gao, W. Fang and Q. Cao, *Molecular Catalysis*, 2017, **439**, 171-179.